IOPscience iopscience.iop.org

Home Search Collections Journals About Contact us My IOPscience

Characteristic length of the glass transition

This article has been downloaded from IOPscience. Please scroll down to see the full text article.

2001 J. Phys.: Condens. Matter 13 L451

(http://iopscience.iop.org/0953-8984/13/22/102)

View the table of contents for this issue, or go to the journal homepage for more

Download details:
IP Address: 94.79.44.176
The article was downloaded on 13/05/2010 at 03:40

Please note that terms and conditions apply.

INSTITUTE OF PHYSICS PUBLISHING JOURNAL OF PHYSICS: CONDENSED MATTER

J. Phys.: Condens. Matter **13** (2001) L451–L462 www.iop.org/Journals/cm PII: S0953-8984(01)20690-0

LETTER TO THE EDITOR

Characteristic length of the glass transition

E Donth, H Huth and M Beiner

Fachbereich Physik, Universität Halle, D-06099 Halle (Saale), Germany

E-mail: donth@physik.uni-halle.de

Received 10 January 2001, in final form 30 April 2001

Abstract

Three lengths for the dynamic glass transition will be compared: a kinematic length from computer simulation, a heterogeneity length from multidimensional nuclear magnetic resonance, and a characteristic length from calorimetry. A qualitatively consistent picture is obtained after discussion of their different origins. The difficulties with respect to measured and simulated lengths are exposed. Heat capacity spectroscopy data for temperatures and frequencies near and above the crossover region of the dynamic glass transition are reported for two substances: poly(*n*-decyl methacrylate), PnDMA, and 6-(4-benzyl oxy phenyl)-1, 2, 3, 4 tetraphenyl fulvene, TPCP-BO.

1. Introduction

The glass transition is an important problem in physics [1] with interest for physical chemistry, biology, materials science, and geology [2,3]. The mystery of the dynamic glass transition is a disengagement of dynamics from structure, i.e. a general, clear architecture of liquid relaxation dynamics in the Arrhenius diagram for glass formers of moderate complexity (figure 1), irrespective of intrinsic complications of the phenomenon and multifarious molecular structures of substances where the traces occur thus or similarly in such diagrams (e.g. silicate glasses, salt melts, metallic glasses, polar liquids, liquid and plastic crystals, polymers). This goes beyond the conventional questions about structure–property relations. No explanation seems possible without knowledge about the typical length scales of dynamic glass transition and their temperature dependence.

Many details about the temporal aspects of liquid dynamics are known, but only a few about the spatial aspects. Recently, the length question came to a head because three long-time efforts yielded seemingly different results:

(i) Molecular dynamics (MD) computer simulations above the crossover region *C* (figure 1) find kinematic lengths relevant for a molecular displacement pattern. They obtained several nanometres, increasing in the direction towards the crossover [4, 5]. At present, MD simulation cannot treat the time range for the α-process, below the crossover in figure 1.

 © 2001 IOP Publishing Ltd Printed in the UK

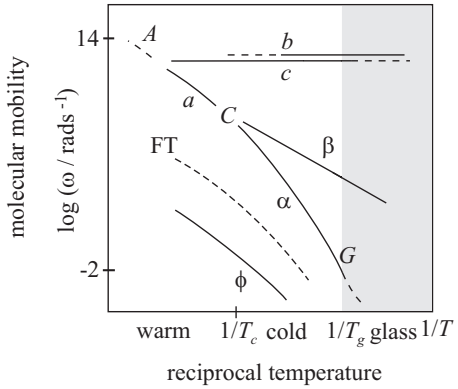

Figure 1. The Arrhenius diagram of liquid dynamics in moderate liquids has a general, clear architecture although the different glass formers have multifarious molecular and liquid structures. A is the molecular transient, a the high-temperature (Williams–Götze) process, b the boson peak, c the cage rattling, C the crossover region, G the thermal glass transition at the glass-transition temperature T_g, T_c the crossover temperature, ϕ the Fischer modes, α the cooperative process, β the Johari–Goldstein process, FT the flow transition (only for polymers). Since the a-process and α-process are distinct and independent, the liquid state for $T > T_c$ is called warm liquid and that for $T_g < T < T_c$ cold liquid. $T < T_g$ (grey) is the glass state below T_g.

(ii) Multidimensional NMR experiments near the conventional glass temperature T_g find heterogeneity lengths relevant for the size of less mobile regions. They obtained one nanometre for glycerol, increasing with decreasing temperature [6].

(iii) Heat capacity spectroscopy (HCS) finds characteristic lengths relevant for an entropy fluctuation pattern. For moderate liquids (see below), the characteristic lengths are about half a nanometre in size and nearly constant above the crossover, and are smaller than the kinematic length there. There is no maximum at the crossover [7]. The characteristic lengths steeply increase up to 1.5–4.0 nanometres below the crossover in the direction towards T_g [8]. The characteristic length for glycerol is larger than the NMR heterogeneity length.

The aim of this paper is to present our new HCS results (figure 2 and details in figures 3 and 4) and to discuss the above differences.

An advantage of the above disengagement of general dynamics from multifarious molecular structure (figure 1) is the comparability of dynamics between different moderate liquids. Lennard-Jones mixtures are accessible to relevant computer simulations above the crossover, at megahertz or gigahertz frequencies, although there is no similar substance available for real glass-transition experiments. The higher poly(n-alkyl methacrylates) (PnAMA) are accessible to relevant HCS above the crossover, although and because the crossover is surprisingly shifted to low frequencies of kilohertz or even hertz order.

This letter is mainly concerned with the dynamics of *moderate liquids*. The term 'moderate' is related to the moderate complexity between simple and normal liquids with unavoidable crystallization, on the one hand, and exceptional glass formers [9], on the other hand. Moderate liquids are thus glass-forming liquids of moderate complexity with a relaxation dynamics characterized by: predominance of similarity, limited individuality, and no exceptional features (as e.g. described by Angell [9]). It is assumed that the Lennard-Jones mixture for computer simulation, glycerol for the NMR experiments, and the poly(n-alkyl methacrylates) for heat capacity spectroscopy belong to the class of moderate liquids, i.e., that

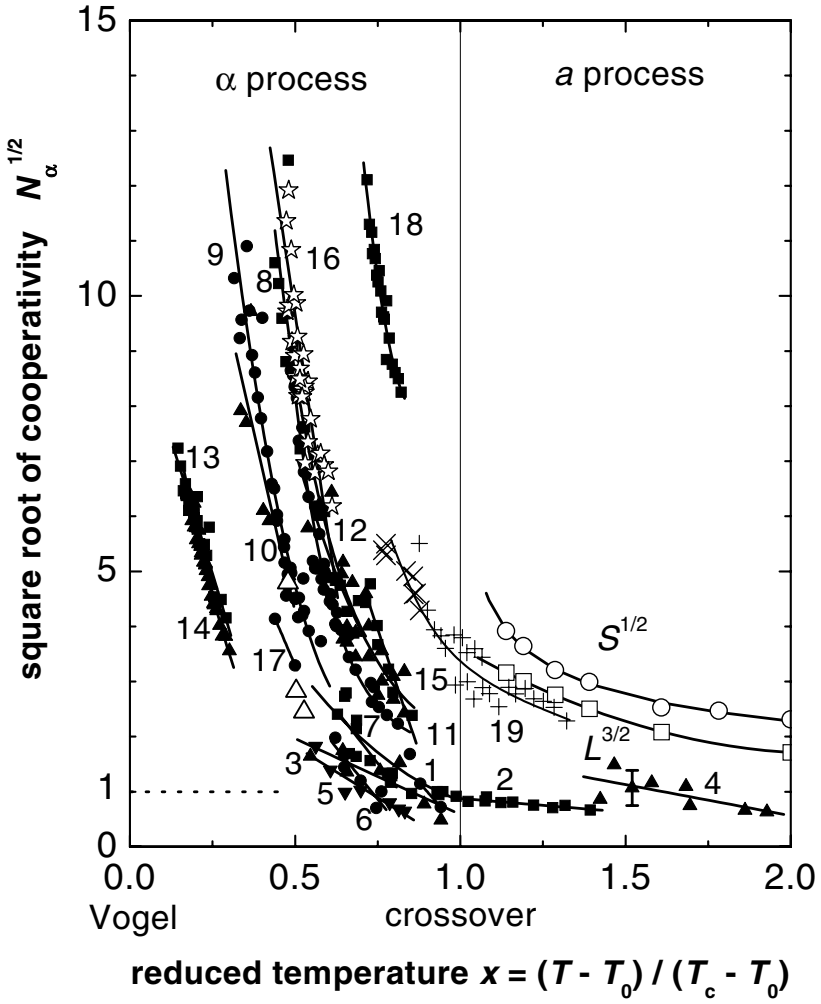

Figure 2. Square root of cooperativity, $N_\alpha^{1/2}(x)$, as a function of reduced temperature $x = (T-T_0)/(T_c-T_0)$; i.e. $x = 0$ for $T = T_0$ and $x = 1$ for $T = T_c$. T_0 is the Vogel temperature from an extrapolation of the α-traces in the Arrhenius diagram by means of a WLF equation from dielectric measurements. T_c is the crossover temperature. $T_0 = 180$ K and $T_c = 240$ K for PnDMA were estimated by an extrapolation from the other PnAMA series members. For the reduced temperature x of the computer simulations we use $T_0 = 0.32$ [29] and $T_c = 0.425$ [5] LJ units. As there are different methods for T_c-determination available [42], the most reliable data and methods are selected individually for each substance. The x-values for OCGE (18) become especially uncertain because there are two β-processes and therefore two possible T_c-values. Using the other T_c, the OCGE trace (18) would be near the polystyrene trace (8). The remaining uncertainty for the other substances is $\Delta T_c \lesssim 10$ K resulting in only small x-uncertainties. The lines are guides for the eyes. Poly(n-alkyl methacrylate) PnAMA series: 1, •, PnOMA; 2, ■, PnHMA; 3, ▲, PnBMA; 4, ▲, PnDMA. Random nBMA styrene copolymers containing: 5, ▼, 2% styrene; 6, •, 8% styrene; 7, ■, 19% styrene. Other substances: 8, ■, polystyrene; 9, •, styrene butadiene rubber (SBR 1500); 10, ▲, natural rubber; 11, ■, bromo isoprene isobutylene rubber (BIIR); 12, •, polyisobutylene; 13, •, diglycidyl ether of bisphenol A (DGEBA, Epon828); 14, ▲, poly[(phenyl glycidyl ether)-co-formaldehyde] (PPGE); 15, ▲, benzoin isobutyl ether (BIBE); 16, open star and △, glycerol (open star from HCS, △ from spin diffusion [6]); 17, •, propylene glycol (PG); 18, ■, ortho cresyl glycidyl ether (OCGE); 19, × and +, 6-(4-benzyl oxy phenyl)-1, 2, 3, 4 tetraphenyl fulvene (TPCP-BO) (× from TMDSC, + from 3ω method). Lennard-Jones mixtures [4,5]: S, ◯, cluster size; L, □, string length (for the reduction to N_a, see the text).

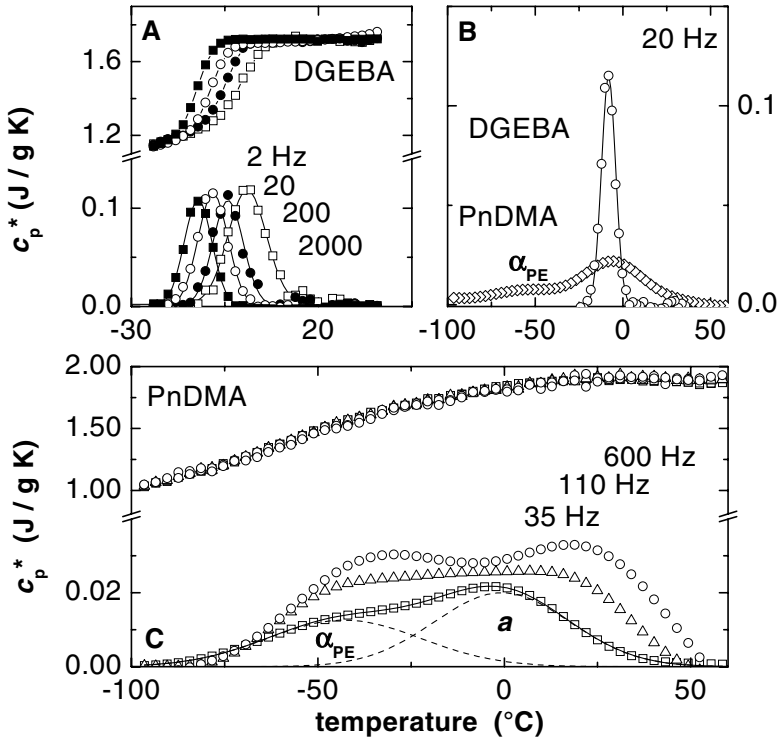

Figure 3. Heat capacity spectroscopy by the 3ω method for DGEBA (Epon828) and poly(n-decyl methacrylate) (PnDMA). Isochronous sections of the $c_p^* = c' - ic_p''$ functions: $c_p^* = c_p^*(\log\omega, T)$; c_p', the real part (top); c_p'', the imaginary part (bottom). The c_p''-data for PnDMA are smoothed by an eight-point fast-Fourier-transformation technique; $c_p''(T)$ was adjusted by a Gauss function, $c_p'' \sim \exp(-(T-T_\omega)^2/2(\delta T)^2)$, from which T_ω was used for temperature T in figure 2, $T = T_\omega$, and δT was used in equation (1) for the calculation of the cooperativity N_α. (**A**) DGEBA at four selected frequencies $\nu = \omega/2\pi$. (**B**) Comparison of DGEBA (α-process) and PnDMA for $\nu = 20$ Hz (a-process and α_{PE}-process). $\delta T_{DGEBA} = 3.1$ K, $\delta T_{PnDMA}^{a\text{-process}} = 15.0$ K, $\delta T_{PnDMA}^{\alpha_{PE}} = 18.3$ K. (**C**) PnDMA at three frequencies. Note that the two peaks for the α_{PE} and α processes are the result of a nanophase separation between alkyl parts of the side chains and relevant 'main chain phase'. For details, see the text. Note the progress in the experimental technique for the 3ω method: the c_p''-peak as typically measured for glass formers is similar to that of DGEBA. The amplitudes for PnDMA are five times smaller and the temperature interval where the complete adhesion of the sample on the nickel heater (70 nm thick) and substrate (PEEK) must be guaranteed is $\Delta T = 170$ K, partly above and partly below the thermal glass transitions.

the architectures (figure 1) and the parameters of their relaxational dynamics are more or less comparable.

HCS data for one more complex substance (TPCP-BO [10]) will be additionally reported (figure 4). This substance has the crossover in the hertz frequency region, obeys the crossover scenario II [11, 12], and is perhaps exceptional.

2. Characteristic lengths from calorimetry?

Figure 2 collects all characteristic lengths for moderate liquids (Nos 1–18) that have been recently obtained by our group in Halle from the 3ω method [13] of HCS. The lengths are expressed by cooperativities N_α, the number of molecules or monomeric units (molecular mass

M_0) in a cooperatively rearranging region CRR [14] of size $V_\alpha = \xi_\alpha^3$, with ξ_α the characteristic length of dynamic glass transition. The cooperativities N_α were calculated from HCS curves using a fluctuation formula [8]:

$$N_\alpha = RT^2\,\Delta(1/c_V)/M_0(\delta T)^2 \approx RT^2\,\Delta c_p/\bar{c}^2 M_0(\delta T)^2 \tag{1}$$

with R the molar gas constant, $\Delta(1/c_V) = (1/c_V)^{\text{glass}} - (1/c_V)^{\text{liquid}}$, the step of reciprocal specific heat capacity at constant volume at the glass transition (c_p is at constant pressure), and $(\delta T)^2$ the mean square temperature fluctuation of one average CRR at temperature T. The uncertainties of the parameters in equation (1) are discussed in reference [15].

We think that the controversies about the determination of a nanoscopic cooperativity from macroscopic calorimetry have now been settled.

(i) The 3ω method determines the complex thermal effusivity, $(\rho\kappa c_p)^*$. The parameters needed for equation (1) come only from the dynamic heat capacity $c_p^* = c_p' - \mathrm{i}c_p''$ and may therefore be influenced by the thermal conductivity κ. However, κ neither shows a frequency dispersion at the dynamic glass transition [16] nor shows a step in its temperature dependence there [17].

(ii) Equation (1) stems from the non-conventional von Laue approach to thermodynamics [18] adapted to glass transition. The alternative formula from the conventional Gibbs distribution yields cooperativities [19] for the glass transitions in confining geometries that are much too large, much larger than any reasonable morphological length such as layer thickness or pore diameter, whereas the characteristic length from equation (1) is consistent with the morphology [19].

(iii) The von Laue approach is based on freely fluctuating representative subsystems inside the sample. These subsystems are defined via a representativeness gedanken experiment [11,20] for determination of subsystems with representative linear response susceptibilities as measured by the fluctuation-dissipation theorem (FDT). The gedanken experiment defines the subsystems in terms of mutual statistical independence of relevant dynamics and uses a partition of the sample into smaller parts. The CRR is the smallest representative freely fluctuating subsystem related to the α-process dynamics. This gedanken experiment is for liquids and has no meaning for all aspects that are connected with translational invariance of crystals. This invariance is not compatible with such a partition into smaller and smaller representative subsystems.

(iv) The specific heat at constant volume has also a dispersion at the dynamic glass transition, $c_V = c_V(\log\omega, T)$. This was experimentally demonstrated by O'Reilly several decades ago [21]: $\Delta c_V \neq 0$; on average we get $\Delta c_V \approx 0.74\,\Delta c_p$ near T_g.

(v) In particular, it seemed questionable to determine the temperature fluctuation δT of a nanometre-sized CRR from a macroscopically obtained width of the $c''(\log\omega, T)$ peak (see, e.g., figure 3). The linear response of a CRR, however, is the same as, i.e. is representative of, that of the whole sample. Intuitively [8], δT was considered as a dispersion partner of a frequency dispersion width across the dynamic glass transition ($\delta\ln\omega$, of course, not depending on subsystem size). This was used in the temperature–logarithm-of-time equivalence, $\mathrm{d}T/\mathrm{d}\ln\omega = \delta T/\delta\ln\omega$, to calculate δT from $\delta\ln\omega$ and the slope along the trace in the Arrhenius diagram, $\mathrm{d}T/\mathrm{d}\ln\omega$. Deeper insights are possible by applying linear response methods using a spectral density for temperature fluctuation allowed by the von Laue approach (see [15], and Example 1 in section 3.3 of [11]).

(vi) Small cooperativities of order $N_\alpha = 1$ can be understood by considering a fluctuating mobility pattern of dynamic heterogeneity ($\log\omega(\boldsymbol{r}, t)$) dense enough [20] for a quasi-continuous treatment in the one-nanometre range [22]. This pattern is given a physical basis for entropy or density fluctuations by considering the FDT as an experimental

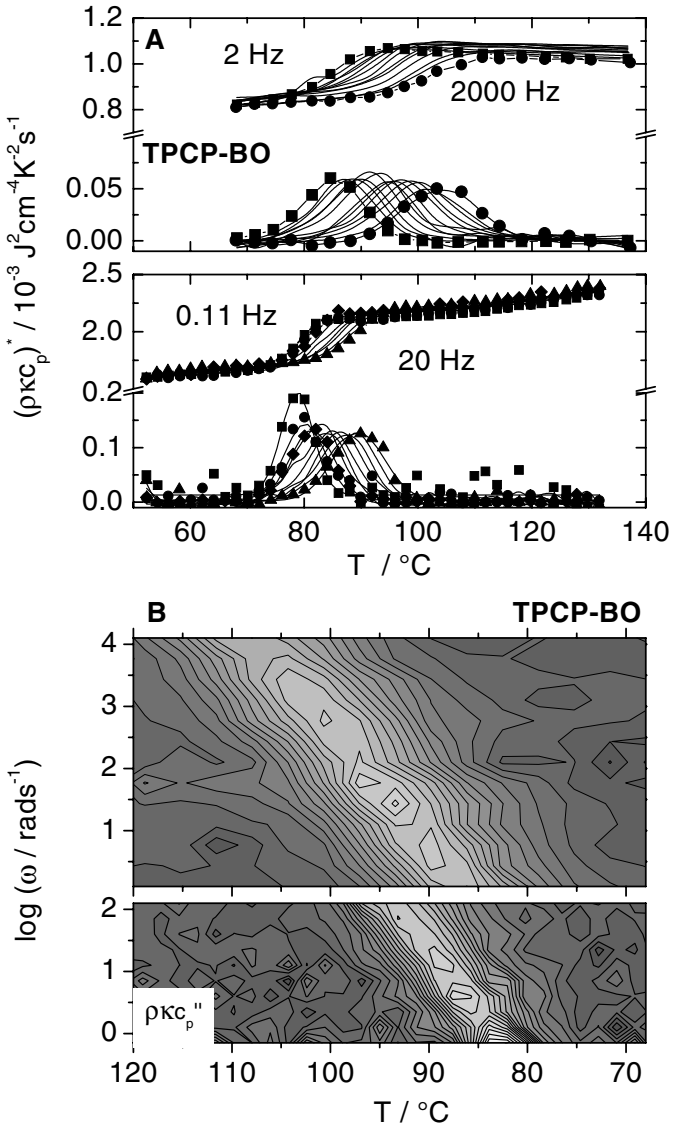

Figure 4. Heat capacity spectroscopy by the 3ω method for TPCP-BO: 6-(4-benzyl oxy phenyl)-1, 2, 3, 4 tetraphenyl fulvene. (**A**) The original real and imaginary outputs of the 3ω method for two runs (*top*, run 1: Ni heater area $= 1.5 \times 5.6$ mm^2; *bottom*, run 2: Ni heater area $= 5 \times 10$ mm^2); $\rho\kappa c_p$ is the thermal effusivity with ρ the mass density, κ the thermal conductivity, and c_p the specific heat capacity. The uncertainties of the N_α- or N_a-calculation from the 3ω-method output are analysed in [41]. Symbols for run 2: ■, 0.11 Hz; •, 0.20 Hz; ♦, 0.36 Hz; ▲, 20 Hz. (**B**) Contour maps of imaginary 3ω-method output in the vicinity of the crossover region. *Top*: run 1; *bottom*: run 2. The 'vertical' scales for run 1 and run 2 are different; a comparison can be made in part (**A**). The true scenario I 'saddle' as for PnHMA [7] is degenerate for this scenario II: no minimum along the ridge and, if any, only a small dislocation between the α- and a-ridges (only visible for run 2). (**C**) Temperature dependences of parameters for TPCP-BO in the vicinity of the crossover region. *Top*, Arrhenius plot: a-process, α-process, β-process. Symbols: □, ■, dielectrics; ◯, calorimetric. *Middle*, dielectric intensity ($\Delta\varepsilon$) and calorimetric intensity (ΔC_p) (step heights; the values of ΔC_p are from the $(\rho\kappa c_p)^*$ outputs, calibrated for each run via comparison with TMDSC by the appropriate constant factor (symbols as for top panel); the left ($\Delta\varepsilon$) and the right (Δc_p) scale are matched for the main transition $= a$- and α-process). *Bottom*, $\delta T =$ average temperature fluctuation of a CRR from calorimetry.

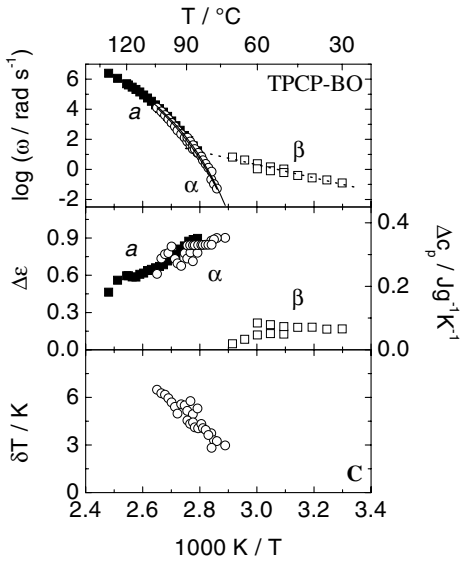

Figure 4. (Continued)

equation, similarly to the approach in an old paper by Nyquist with quanta $\hbar\omega$ in his transmission line model [23]. Equation (1) and the possibility of obtaining such small cooperativities are related to the disengagement of dynamics from structure.

(vii) Above the crossover, a model for a characteristic length of half a nanometre ($N_a \approx 1$) is based on 'escaping the cage' as described by Götze's mode-coupling theory and by computer simulation. 'Escaping' means diffusion through a fluctuating 'cage door' [11] formed by cooperative movements of equivalent neighbour molecules. Such fluctuations are relevant for entropy fluctuations detected by HCS. Because of the shortage of free volume for the a-process also, for moderate liquids this fluctuation is concentrated in the volume of a cage door just of the size of the escaping molecule ($N_a = 1$). The volume V_a is the primary experimental result from equation (1).

(viii) An independent consistency argument for the characteristic length as obtained from the von Laue approach comes from low-temperature calorimetry in the 1 K range. The density of tunnelling systems as a function of the n-alkyl side-group length in the poly(n-alkyl methacrylate) PnAMA series shows a large maximum (factor six) [24] just for that length where the decreasing cooperativity $N_\alpha(T_g)$ along the series passes the number of monomeric units in the first coordination shell: the tunnel density increases first due to an increasing number of (smaller) CRRs and breaks down when $N_\alpha(T_g)$ decreases below a minimal number needed to form a vault around the one Glarum defect of each CRR promoting the tunnelling system [11, 22, 24]. For the alternative Gibbs formula we had to explain this vault breakdown effect with about 500 (instead 15) particles or monomeric units.

(ix) The Mainz school of glass transition [25] 'will call a system dynamically heterogeneous if it is possible to select a dynamically distinguishable subensemble by experiment or computer simulation'. This definition may be concentrated on selectability and can do without spatial aspects. Moreover, they claim [26] that 'a strict distinction between the heterogeneous and homogeneous scenarios requires comparison of two-time and three-time correlation functions'. This could exclude dynamic scattering [27] from the

length discussion (!). Such an exclusion does not seem necessary since length information can also be obtained from a comparison of different activities from linear response investigations, e.g. of dynamic neutron scattering and dielectrics [28]. Furthermore, 'the very basis of the representative subsystems ... is not easily reconciled with a heterogeneous [25] scenario where dynamically distinct subsystems can be selected and only sets of such different subsystems can represent the whole system' [43]. We think that (a) Glarum defects (the islands of mobility) and (b) their environments (the cooperativity shells)—both a consequence [11] of the representativeness concept—may be interpreted as dynamically distinct subensembles in the sense of reference [25]. In our sense [11] a CRR consists of Glarum defect and cooperativity shell. The relationship between representative subsystems and dynamic heterogeneity will be discussed in detail elsewhere [11].

3. Comparison of lengths from computer simulation, multidimensional NMR methods, and heat capacity spectroscopy

3.1. Data transfer to the cooperativity–temperature plot

The kinematic lengths from MD computer simulation are transferred to the $N_a^{1/2}(x)$ plot (figure 2) as follows. The reduced temperatures $x = (T - T_0)/(T_c - T_0)$ were calculated using a Vogel temperature, $T_0 = 0.32$ Lennard-Jones units [29], and using a crossover temperature of $T_c = 0.435$ [4]. The 'cooperativity' N_a for the mean cluster size S was set as $N_a = S$; for the mean string length L we put $N_a = L^3$, assuming one particle in a Lennard-Jones unit cube.

The characteristic cooperativity N_a above the crossover region has been determined so far for two moderate polymers, No 2 and No 4 of figure 2, and for the more complicated glass former TPCP-BO (No 19). The data for the hexyl PnAMA member, PnHMA, 2, were taken from reference [7]. For calculation of the cooperativity for the decyl member, PnDMA, 4, we used a correction from a black-and-white depiction of the nanophase separation [30] in polymers with long side chains. We assume, arbitrarily, that the octyl rests of the side chains contribute to the glass transition [31] in the PE nanophase (α_{PE}), and the other (the relevant) glass transition (figure 3) is caused by the ethyl rests together with the main chain units (PEMA nanophase). This gives unique phase fractions $f < 1$ for $\Delta c_p \rightarrow \Delta c_p/f$ and new molecular masses M_0, both for correcting equation (1) for the two glass transitions. The uncertainty of the $N_\alpha^{1/2}(x)$ points for PnDMA is larger than usual (20%); we estimate $\pm 30\%$ of $N_\alpha^{1/2}$. We assume that the dynamic glass transitions make, for increasing mobility $\log \omega$ or increasing temperature T, the corresponding monomeric units mobile for a limited diffusion through the cage door before the flow is restricted due to the macromolecular chains [32] and due to the nanophase boundaries, both becoming effective at longer scales. Such models seem of relevance for the glass transition in native proteins [33] having probably a separation into several nanophases.

As mentioned above, TPCP-BO was selected for HCS calorimetry because the crossover region is in the $\omega = 10$ rad s^{-1} range and the crossover region is therefore accessible using our 3ω-method equipment. The glass temperature is $T_g \approx 85$ °C. The chemical structure (figure 5) has an 'anchor' R that may entangle with several a-process cage particles, so a cage door larger than $N_a = 1$ is expected for the particle diffusion. This suggests also a larger cage and, therefore, not so large a difference between the a-process and α-process (scenario II). The data (figure 4) show that $N_a \approx 10$ is obtained near the crossover temperature (No 19), falling in the direction towards higher temperatures in the warm liquid. The entanglement by the R anchor may also be responsible for the low crossover frequency.

Some details of the experiments and evaluation are described in the caption of figure 4.

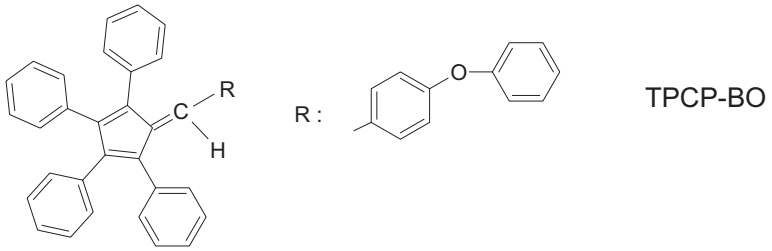

Figure 5. The chemical structure of TPCP-BO.

The synthesis is a complicated multi-step procedure [34]. Comparing different TPCP-BO samples we observed small differences in the relaxation behaviour, namely a difference in a-, α-, and β-process frequencies of less than one decade. Our presented data are for the sample with the best stability having reproducible glass-transition temperature T_g.

3.2. Comparison of the different lengths

The difference between the kinematic MD simulation lengths (from S and L) and the characteristic HCS lengths above the crossover region (ξ_a) will be explained by the following argument. Obviously neither the kinematic correlations leading to the mean cluster size S nor the string combinations leading to the mean string lengths L are as a whole connected with an entropy fluctuation. Kinematic correlations contain also correlations with no entropy fluctuation (example: parallel displacements), so the pattern of entropy fluctuation is expected to be more finely granulated, consistently with the HCS findings [20].

For further explanation of the relation between kinematic and characteristic lengths we use the term 'factual', i.e. relating to facts accessible by experiments. For factual entropy fluctuations we need large amplitudes of disordered molecular moves that can really change the weights of different configurations responsible for local entropy fluctuation. In this sense opening the cage door seems entropy active, but collective distortions of the cage, with small molecular amplitudes, also necessary for the cage-escaping a-process, do not seem entropy active. For the strings, we see two extreme possibilities. Either the string molecules move collectively, as if through a tube (not entropy active), or the molecules move as a succession of individual cage-door openings. The latter corresponds, in moderate liquids, to $N_a = 1$ with the above factual and individual entropy fluctuations.

The above comparison is made via numbers of particles N_a. This reflects the fact that it is, at the moment, one particle that diffuses through the a-process cage door in moderate liquids. The comparison of Lennard-Jones particles with polymer monomeric units is based on two features: the generality of the relaxation chart of figure 1, connected with the disengagement of the mobility pattern from structure, and the thermodynamic independence of monomeric units as relevant for the main transition in polymers. The latter is, by the way, also expressed by the Flory–Huggins formula for polymer mixtures.

Moreover, the map from computer kinematics to thermodynamics may be influenced by von Laue temperature fluctuations (δT) missing in the Gibbs distribution (see below, and also [11], section 3.2). This map may also be complicated by an average distance between simultaneously active escape-the-cage events. Change of this distance, e.g. with temperature, is not active for entropy fluctuation as long as, above T_c, all molecules are dynamically equivalent. The kinematic lengths are, therefore, not directly related to 'cooperatively rearranging groups' when the term rearranging is connected with fluctuations of thermodynamic variables as Adam

and Gibbs intended.

A certain effect of the larger kinematic length, however, is probably related to an experimental finding for the glass transition in confining geometries [35, 36]—namely, that the characteristic length for the α-process is sensitive to decrease of pore radius or layer thickness at lengths larger than ξ_α.

In general, the transferability of MD computer simulation to experimental linear response and dynamic scattering results depends on whether or not the von Laue approach must be used. On the one hand, the temperature fluctuation δT transfers different states to the average. This may result in a sharpening of traces in the Arrhenius diagrams. The energy fluctuation, on the other hand, may result in the opposite: smoothing of the traces in this diagram. This difference would be crucial in the crossover region with δT of order 20 K.

The transfer via the von Laue approach may be 'measured' in the MD simulation results analogously to the steps of reasoning for the von Laue approach [11, 18, 20]: find first the smallest freely fluctuating representative subsystem for the a-process or α-process and try then to introduce the mechanics in a 'microscopic von Laue distribution' by input of minimal work. A simpler test would be to check whether in a molecular–mechanical model for a truly two-dimensional thermodynamic situation (e.g. $\mathrm{d}U = T\,\mathrm{d}S - p\,\mathrm{d}V$) either $k_B C_p = \overline{\Delta H^2}/T^2$ (as for Gibbs) or $k_B C_p = \overline{\Delta S^2}$ (as for von Laue) is obtained, with

$$H = U + pV = \text{enthalpy} \qquad C_p = (\partial H/\partial T)_p$$

for both. This test needs a definition of local energy, entropy (or temperature), and density fluctuations on the CRR scale.

All substances that we have measured by the 3ω method of HCS (and, by the way, also those measured by temperature-modulated differential scanning calorimetry, TMDSC) show a steep increase of cooperativity below the crossover (figure 2). Inversely, apart from that on the non-moderate TPCP-BO (No 19), all experiments were on moderate liquids and led (partly in the extrapolation) to small cooperativities of order $N_\alpha = 1$ near the crossover, consistent with the two examples of $N_a \approx 1$ cooperativities measured above the crossover (Nos 2 and 4 in figure 2). Apart from for No 19, we observed no clear counterexample for this $N_\alpha(T)$ behaviour. This means that the α-process below the crossover and the a-process above the crossover (the Williams–Götze process) are really independent and distinct processes (as conjectured by Williams several decades ago [37]). The main difference is the steep increase of cooperativity for the α-process (as conjectured by Johari also several decades ago [38]) when compared to the (weakly decreasing but) small cooperativity of the a-process. The usually large cooperativity of the α-process near T_g ($N_\alpha(T_g) = 30$–300 [8, 15]) is consistent with indications from many other experiments (there are reviews by Sillescu [39] and Ediger [40]).

The heterogeneity lengths, being the diameters of the less mobile regions in glycerol [6] as determined from spin-diffusion tests of spin correlations by multidimensional NMR experiments, fit into the general trend of figure 2 (△). They may be reconciled with our larger CRR sizes (★, open star, 16), since the less mobile regions are only a fraction of each CRR. Each CRR also includes one island of mobility [22], a more mobile region. The heterogeneity lengths from NMR alone, apart from the comparison with characteristic lengths from HCS, would, in the extrapolation, also be confronted with the problem of small lengths of order half a nanometre in the crossover region.

The general trend of the figure 2 traces is consistent with the disengagement concept. The distribution of these traces (the longer curves correspond to a common HCS frequency window between about 1 Hz and 10^3 Hz) reflects some material individuality of the nanometric subsystems.

The overall experimental situation will be improved when, perhaps in five years, for

substances with the crossover region in the megahertz range, the length information contained in dynamic neutron or x-ray scattering overlaps with the length information contained in HCS (periodic calorimetry). We think that this will be the *experimentum crucis* of dynamic glass transition, deciding experimentally about the necessity of using a non-conventional thermodynamics, the physical essence of the crossover region, and the reliability of the disengagement concept.

4. Conclusions

In summary, accepting that the three lengths for the dynamic glass transition come from different activities and assuming that the relevant substances belong to the substance class of glass formers with moderate complexity, their comparison gives a qualitatively consistent picture. The large characteristic length of several nanometres at the glass temperature T_g in the cold liquid steeply decreases to values of about half a nanometre in the crossover region. Above the crossover, the characteristic lengths in the warm liquid remain approximately constant. There is no singularity of characteristic length at the crossover temperature.

Our former colleagues Stefan Kahle, Jörg Korus, Sven Reissig, and Kerstin Gutewort have done some experimental work for several substances included in figure 2. We thank Professor D Braun from Deutsches Kunststoff-Institut (Darmstadt) for providing the TPCP-BO sample, Professor A Heuer for the discussion of a preliminary draft of the manuscript, and the Deutsche Forschungsgemeinschaft DFG (SFB 418) and the Fonds Chemische Industrie FCI for financial support.

References

[1] Anderson P W 1995 *Science* **267** 1615
[2] Angell C A 1995 *Science* **267** 1924
[3] Frick B and Richter D 1995 *Science* **267** 1939
[4] Donati C, Douglas J F, Kob W, Plimpton S J, Poole P H and Glotzer S C 1998 *Phys. Rev. Lett.* **80** 2338
[5] Glotzer S C 2000 *J. Non-Cryst. Solids* **274** 342
[6] Reinsberg S A, Qiu X H, Wilhelm M, Spiess H W and Ediger M D 2001 *J. Chem. Phys.* **114** 7299
[7] Beiner M, Kahle S, Hempel E, Schröter K and Donth E 1998 *Europhys. Lett.* **44** 321
[8] Donth E 1982 *J. Non-Cryst. Solids* **53** 325
[9] Angell C A 2000 *Solid State Sci.* **2** 791
[10] Huth H 2001 *PhD Thesis* Universität Halle
[11] Donth E 2001 *The Glass Transition. Relaxation Dynamics in Liquids and Disordered Materials* (Heidelberg: Springer)
[12] Kahle S, Schröter K, Hempel E and Donth E 1999 *J. Chem. Phys.* **111** 6462
[13] Birge N O and Nagel S R 1985 *Phys. Rev. Lett.* **54** 2674
[14] Adam G and Gibbs J H 1965 *J. Chem. Phys.* **43** 139
[15] Hempel E, Hempel G, Hensel A, Schick C and Donth E 2000 *J. Phys. Chem.* B **104** 2460
[16] Dixon P K and Nagel S R 1988 *Phys. Rev. Lett.* **61** 341
[17] Huth H, Beiner M and Donth E 2000 *Phys. Rev.* B **61** 15 092
[18] von Laue M 1917 *Phys. Z.* **18** 542
Landau L D and Lifshitz E M 1980 *Statistical Physics (Course of Theoretical Physics vol 5)* 3rd edn (Oxford: Pergamon) §112
[19] Donth E, Hempel E and Schick C 2000 *J. Phys.: Condens. Matter* **12** L281
[20] Donth E 2000 *J. Phys.: Condens. Matter* **12** 10 371
[21] O'Reilly J M 1962 *J. Polym. Sci.* **57** 429
[22] Donth E 1999 *Acta Polym.* **50** 240
[23] Nyquist H 1928 *Phys. Rev.* **32** 110
[24] Beiner M, Kahle S, Abens S, Hempel E, Höring S, Meissner M and Donth E 2001 *Macromolecules* submitted

[25] Böhmer R, Chamberlin R V, Diezemann G, Geil B, Heuer A, Hinze G, Kuebler S C, Richert R, Schiener B, Sillescu H, Spiess H W, Tracht U and Wilhelm M 1998 *J. Non-Cryst. Solids* **235–237** 1
[26] Heuer A and Spiess H W 1999 *Phys. Rev. Lett.* **82** 1335
[27] Arbe A, Colmenero J, Monkenbusch M and Richter D 1999 *Phys. Rev. Lett.* **82** 1336
[28] Kahle S 1999 private communication
[29] Coluzzi B, Parisi G and Verrocchio P 2000 *Phys. Rev. Lett.* **84** 306
[30] Chen W and Wunderlich B 1999 *Macromol. Chem. Phys.* **200** 283
[31] Heijboer J and Pineri M 1982 *Non-Metallic Materials and Composites at Low Temperatures 2* ed G Hartwig and D Evans (New York: Plenum) p 89
[32] Baschnagel J, Bennemann C, Paul W and Binder K 2000 *J. Phys.: Condens. Matter* **12** 6365
[33] Sartor G, Mayer E and Johari G P 1994 *Biophys. J.* **66** 249
[34] Langendorf R 1997 *PhD Thesis* Universität Darmstadt
[35] Hempel E, Huwe A, Otto K, Janowski F, Schröter K and Donth E 1999 *Thermochim. Acta* **337** 163
[36] Schick C and Donth E 1991 *Phys. Scr.* **43** 423
[37] Williams G 1965 *Trans. Faraday Soc.* **61** 1564
[38] Johari G P 1972 *Faraday Symp. Chem. Soc.* **6** 42
[39] Sillescu H 1999 *J. Non-Cryst. Solids* **243** 81
[40] Ediger M D 2000 *Annu. Rev. Phys. Chem.* **51** 99
[41] Huth H, Beiner M, Weyer S, Merzlyakov M, Schick C and Donth E 2001 *Thermochim. Acta* at press
[42] Beiner M, Huth H and Schröter K 2001 *J. Non-Cryst. Solids* **279** 126
[43] Unknown referee for the final version of this letter.